SUPPORTING INFORMATION

SPREADING KINETICS OF ULTRA-THIN LIQUID FILMS USING MOLECULAR DYNAMICS

Brooklyn A. Noble[1], C. Mathew Mate[2], and Bart Raeymaekers[1,*]

[1]Department of Mechanical Engineering, University of Utah, Salt Lake City, UT 84112, USA

[2]1672 Hester Ave., San Jose, CA 95128, USA

Potential function interactions. Figure S1 (a) and (b) depict the potential function interactions for Zdol and Z molecules, respectively, using the corresponding equation numbers, and are similar to validated potentials and parameters used in previous research.[32,36-38] A truncated, shifted Lennard Jones potential U_{LJ} exists between all polymer beads, given by

$$U_{LJ}(r) = 4\varepsilon\left[\left(\frac{\sigma}{r}\right)^{12} - \left(\frac{\sigma}{r}\right)^{6} - \left(\frac{\sigma}{r_c}\right)^{12} + \left(\frac{\sigma}{r_c}\right)^{6}\right], \quad (1)$$

where r is the distance between two beads, σ = 0.7 nm is the bead diameter, $r_c = 2.5\sigma$ is the cutoff distance within which interactions between neighboring beads are considered, and $\varepsilon = Tk_B$ is the potential well depth, where T = 300 K is the absolute temperature and k_B is the Boltzmann constant. A finitely extensible nonlinear elastic (FENE) potential U_{FENE} acts as a spring to bond neighboring beads of the same molecular chain, *i.e.*,

$$U_{FENE}(l) = -\frac{1}{2}kR_0^2 \ln\left[1 - \left(\frac{l - l_0}{R_0}\right)^2\right], \quad (2)$$

where l is the bond length, $l_0 = 1.3\sigma$ is the equilibrium bond length, $R_0 = 0.3\sigma$ indicates the maximum extensible range, and $k = 40\varepsilon/\sigma^2$ is the spring constant. The substrate interacts with the polymer molecules, and attracts polymer backbone beads via a dispersive van der Waals interaction $U_{bb\text{-}wall}$, described as

$$U_{bb-wall}(z) = 4\varepsilon\left[\frac{1}{2}\left(\frac{\sigma}{z}\right)^{9} - \frac{3}{2}\left(\frac{\sigma}{z}\right)^{3}\right], \quad (3)$$

where z is the distance between a substrate bead and a polymer bead. We use a short-range exponential potential $U_{eb\text{-}eb}$ to model the attraction of functional end beads to each other,

$$U_{eb-eb}(r) = -2\varepsilon \exp\left(-\frac{r - r_c}{d}\right), \tag{4}$$

where $r_c = 1.0\sigma$ is the cutoff distance and $d = 0.3\sigma$ is the decay length. Additionally, a fraction of the substrate beads is functional, and an attractive force exists between functional substrate and functional polymer beads, also modeled by a short-range exponential potential $U_{eb\text{-}wall}$,

$$U_{eb-wall}(z) = -2\varepsilon \exp\left(-\frac{z - z_c}{d}\right), \tag{5}$$

where $z_c = 1.165\sigma$ is the cutoff distance.

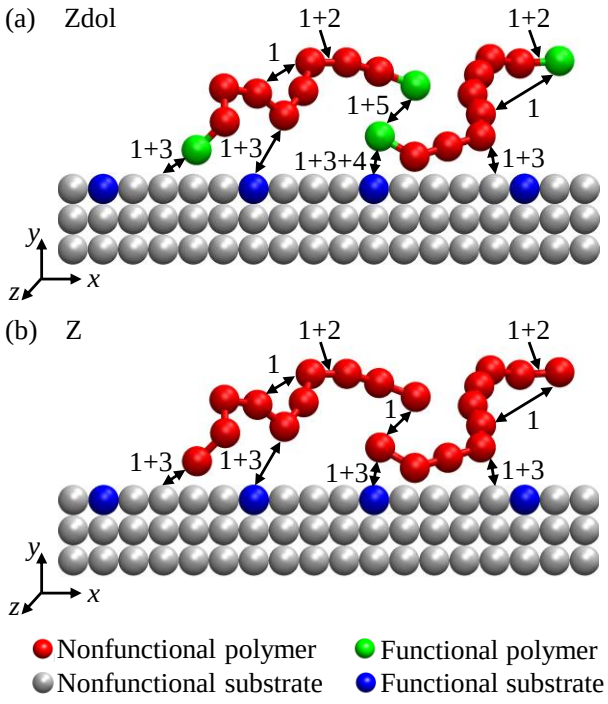

Figure S1. Schematic of potential function interactions for (a) Zdol and (b) Z polymer, with numbers referring to the corresponding equations.

Lubricant displacement maps. Figure R1 shows lubricant displacement D/σ maps at the beginning (200,000-300,000 $d\tau$) and end of the simulation (7,800,000-7,900,000 $d\tau$), averaged along the radial coordinate. From Figure R1, we observe that significant wall slip occurs when the spreading regime is fast $R \sim t^{1/3}$ [(a), (b), (d)], indicated as significant molecule displacement (red) close to the wall. In contrast, wall slip is minimal when the spreading regime is slow $R \sim t^{1/10}$ [(c), (e), (f)], indicated by minimal molecule displacement close to the wall. We note that Tanner's law assumes no wall slip and believe that this may be why the spreading behavior is similar to Tanner's prediction for our simulations when slip is minimal.

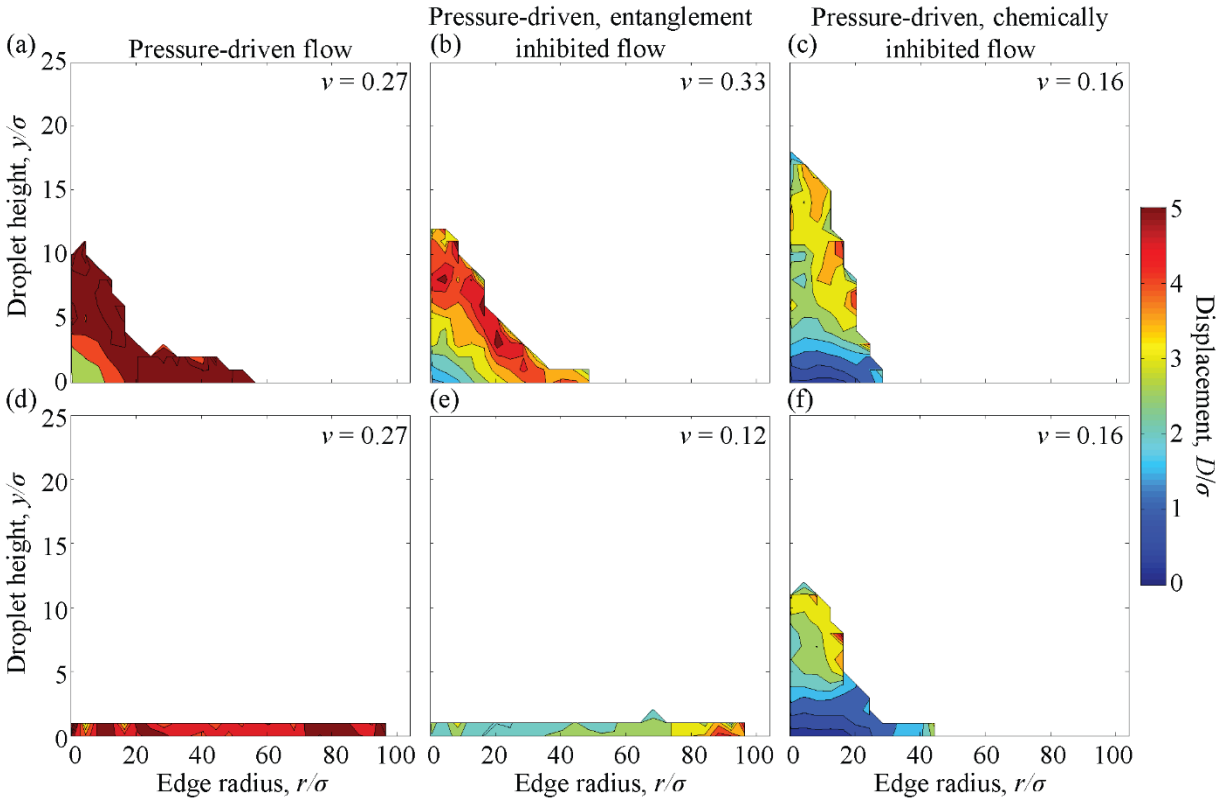

Figure S2. Lubricant displacement maps at the beginning (200,000-300,000 $d\tau$) (a) – (c) and end (7,800,000-7,900,000 $d\tau$) of the simulation (d) – (f) averaged along the radial coordinate, showing pressure-driven flow (Z, N = 10, Q = 10,000), pressure-driven entanglement inhibited flow (Z, N = 400, Q = 10,000), and pressure-driven chemically inhibited flow (Zdol, N = 10,Q = 10,000, S_f = 100%).

Effect of droplet volume. Figure S3 shows the droplet edge radius as a function of time for Z polymer with N = 400 beads/molecule, for different quantities 5,000 ≤ Q ≤ 40,000 of polymer beads,

illustrating a range of droplet volumes. Insets show the droplet thickness profiles for Q = 10,000 (the vertical scale is 10 times larger than the horizontal one, for clarity). From Fig. S3, we observe that the spreading exponent increases slightly with increasing droplet volume, and for Q = 40,000 we do not observe a transition from fast to slow spreading regime because the central droplet does not deplete within the simulation time. We observe similar trends for the entire range of polymer and substrate parameters we consider in this work. We speculate this trend would continue for increasing quantity, converging to a finite value at the macroscopic scale, exemplifying the unique properties of ultra-thin films compared to macroscopic films.

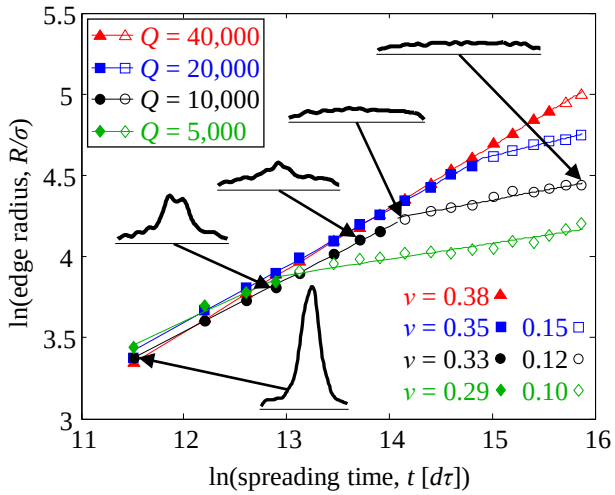

Figure S3. Effect of liquid polymer droplet volume for constant Z molecule length (N = 400). Edge radius versus spreading time where solid and hollow markers indicate that a central droplet exists or has depleted, respectively. Insets show the droplet profiles for Q = 10,000 at the indicated times.

Spreading exponents for all simulations. Table S1 shows the spreading exponents for Z lubricant with molecule length $10 \leq N \leq 400$ and lubricant quantity $5{,}000 \leq Q \leq 40{,}000$, supplementing the spreading exponent values reported in Fig. 2 and Fig. 3. We characterize spreading kinetics in some cases using one spreading exponent (v_1) whereas in other cases we use two spreading exponents that occur sequentially (v_1 followed by v_2). From Table S1, we observe pressure-driven flow (red) characterized by a single, fast spreading speed $v \approx 1/3$ for molecules $N < 50$, corresponding to Fig. 2. For molecules $N \geq 50$, we observe pressure-driven, entanglement inhibited flow (black) characterized by a transition in spreading speed from

fast $v \approx 1/3$ when the central droplet is present, to slow $v \approx 1/10$ after the central droplet depletes, corresponding to Fig. 3. For some cases with $N \geq 50$ but small lubricant quantity (Q = 5,000), we only observe a slow spreading speed because the central droplet depletes almost instantaneously after spreading starts. For cases with $N \geq 50$ and large lubricant quantity (Q = 40,000), we only observe a fast mechanism because the droplet depletes near the end of the simulation (250 ns).

Table S1. Spreading exponents for Z lubricant

N	Q	v_1	v_2
10	5,000	0.27	-
	10,000	0.27	-
	20,000	0.32	-
	40,000	0.37	-
20	5,000	0.27	-
	10,000	0.29	-
	20,000	0.32	-
	40,000	0.36	-
50	5,000	0.16	-
	10,000	0.32	0.15
	20,000	0.34	0.13
	40,000	0.32	-
100	5,000	0.13	-
	10,000	0.28	0.14
	20,000	0.28	0.16
	40,000	0.38	-
200	5,000	0.29	0.10
	10,000	0.34	0.14
	20,000	0.30	0.15
	40,000	0.37	-
400	5,000	0.29	0.10
	10,000	0.33	0.12
	20,000	0.35	0.15
	40,000	0.38	-

Table S2 shows the spreading exponents for Zdol lubricant with functional substrate fraction S_f = 100%, molecule length $10 \leq N \leq 400$, and lubricant quantity $5{,}000 \leq Q \leq 40{,}000$. We characterize spreading kinetics in some cases using one spreading exponent (v_1) whereas in other cases we use two spreading exponents that occur sequentially (v_1 followed by v_2). From Table S2 we observe pressure-driven, chemically inhibited flow (blue), characterized by a single, slow spreading speed $v \approx 1/10$ for $N < 100$, corresponding to Fig. 4. For $N \geq 100$, we observe pressure-driven, entanglement inhibited flow (black) characterized by a transition in spreading speed from fast $v \approx 1/3$ to slow $v \approx 1/10$ after the central droplet

depletes, corresponding to Fig. 3. For some cases with $N \geq 100$ but small lubricant quantity (Q = 5,000), we only observe a slow spreading speed because the central droplet depletes almost instantaneously after spreading starts. For cases with $N \geq 100$ and large lubricant quantity (Q = 40,000), we only observe a fast mechanism because the droplet depletes near the end of the simulation.

Table S2. Spreading exponents for Zdol lubricant with S_f = 100%

N	Q	v_1	v_2
10	5,000	0.12	-
	10,000	0.16	-
	20,000	0.15	-
	40,000	0.12	-
20	5,000	0.16	-
	10,000	0.16	-
	20,000	0.15	-
	40,000	0.16	-
50	5,000	0.15	-
	10,000	0.15	-
	20,000	0.13	-
	40,000	0.15	-
100	5,000	0.11	-
	10,000	0.16	-
	20,000	0.31	0.16
	40,000	0.30	0.16
200	5,000	0.27	0.10
	10,000	0.28	0.13
	20,000	0.29	0.12
	40,000	0.30	-
400	5,000	0.32	0.10
	10,000	0.34	0.11
	20,000	0.34	0.14
	40,000	0.35	-

Table S3 shows the spreading exponents for Zdol lubricant with functional substrate fraction S_f = 0%, molecule length $10 \leq N \leq 400$, and lubricant quantity $5{,}000 \leq Q \leq 40{,}000$. We characterize spreading kinetics in some cases using one spreading exponent (v_1) whereas in other cases we use two spreading exponents that occur sequentially (v_1 followed by v_2). From Table S3 we observe pressure-driven flow (red) characterized by a single, fast $v \approx 1/3$ spreading speed for $N < 50$, corresponding to Fig. 2. For molecules $N \geq 50$, we observe pressure-driven, entanglement inhibited flow (black) characterized by a transition in spreading speed from fast $v \approx 1/3$ to slow $v \approx 1/10$ after the central droplet depletes, corresponding to Fig. 3.

Table S3. Spreading exponents for Zdol lubricant with S_f = 0%

N	Q	v_1	v_2
10	5,000	0.29	-
	10,000	0.30	-
	20,000	0.33	-
	40,000	0.38	-
20	20,000	0.30	-
50	20,000	0.30	0.16
100	20,000	0.29	0.15
200	20,000	0.30	0.14
400	10,000	0.29	0.13
	20,000	0.35	0.16

Video supplements of spreading. We have included three videos of lubricant spreading to supplement Figures 2-4. Each video shows, as a function of time, the plot of droplet edge radius (top left), a side view of the lubricant droplet (bottom left), the entanglement map (top right), and the pressure map (bottom right, the vertical scale is 10 times larger than the horizontal one, for clarity). We illustrate three specific cases. Video S1 shows pressure-driven flow of Z lubricant with molecule length N = 10 beads/molecule and lubricant quantity Q = 10,000 polymer beads, illustrating a case with only a fast spreading speed (v = 0.27) as no functional end groups attach to the substrate or molecule entanglement inhibits spreading. Video S2 shows pressure-driven, entanglement inhibited flow of Z lubricant with molecular chain length N = 400 beads/molecule and lubricant quantity Q = 10,000 polymer beads, illustrating a case in which the lubricant central droplet depletes, resulting in a transition in spreading speed (initial fast spreading speed v = 0.33 followed by a slow spreading speed v = 0.12). Video S3 shows pressure driven, chemically inhibited flow of Zdol lubricant with functional substrate fraction S_f = 100%, molecular chain length N = 10 beads/molecule, and lubricant quantity Q = 10,000 lubricant beads, illustrating a case with only a slow spreading speed (v = 0.16) caused by functional end bead pinning.